

In-flight dissipation as a mechanism to suppress Fermi acceleration.

Diego F. M. Oliveira and Marko Robnik

CAMTP - Center For Applied Mathematics and Theoretical Physics
University of Maribor - Krekova 2 - SI-2000 - Maribor - Slovenia.

(Dated: October 31, 2018)

Some dynamical properties of time-dependent driven elliptical-shaped billiard are studied. It was shown that for the conservative time-dependent dynamics the model exhibits the Fermi acceleration [Phys. Rev. Lett. 100, 014103 (2008)]. On the other hand, it was observed that damping coefficients upon collisions suppress such phenomenon [Phys. Rev. Lett. 104, 224101 (2010)]. Here, we consider a dissipative model under the presence of in-flight dissipation due to a drag force which is assumed to be proportional to the square of the particle's velocity. Our results reinforce that dissipation leads to a phase transition from unlimited to limited energy growth. The behaviour of the average velocity is described using scaling arguments.

PACS numbers: 05.45.Ac, 05.45.Pq

Dissipative systems have attracted much attention during the last years since they can be used in order to explain different physical phenomena in different fields of science including atomic and molecular physics [1, 2], turbulent and fluid dynamics [3–5], optics [6, 7], nanotechnology [8, 9], quantum and relativistic systems [10, 11]. Different procedures can be used to describe such systems. The billiard models are often considered since they can be easily described mathematically and can be realized experimentally in many different ways, for example, the microwave resonators initiated by H.-J. Stöckmann in 1990 [12] and also superconducting microwave resonators [13], quantum dots [14], ultracold atoms [15] and many others. From the mathematical point of view, a billiard is defined by a connected region $Q \subset R^D$, with boundary $\partial Q \subset R^{D-1}$ which separates Q from its complement. If $\partial Q = \partial Q(t)$ the system has a time-dependent boundary and it can exchange energy with the particle upon collision. In such a case, it is possible to investigate the phenomenon called Fermi acceleration, i.e., the unlimited energy growth [16]. According to Loskutov-Ryabov-Akinshin (LRA) conjecture [17], a chaotic component in the phase space with static boundary is a sufficient condition to observe Fermi acceleration when a time dependent perturbation is introduced. Results that corroborate the validity of this conjecture include the time dependent oval billiard [18, 19], stadium billiard [20], Lorentz Gas [21]. Recently, it was shown even that a specific perturbation in the boundary of an elliptical billiard (integrable) leads to the unlimited energy growth [22]. The separatrix gives place to a chaotic layer and the particles can now experience unlimited energy growth while diffusing in the chaotic layer.

In this Letter, we will consider a dissipative elliptical billiard with a periodically moving boundary which has been studied in the pioneering paper in 1996 [24]. Firstly, we assume that the particles of mass m are immersed in a fluid. The dissipative drag force is considered to be proportional to the square of the velocity of the particle, \vec{V} . To obtain the equation that describes the velocity of the particle along its trajectory, we need

to solve Newton's equation where $m d\vec{V}/dt = -\eta' \vec{V}^2$ with the initial velocity $\vec{V}_n > 0$ and η' is the coefficient of the drag force. After we introduce the variables $\eta'/m = \eta$, we obtain the velocity of the particle as function of time as $\vec{V}_p(t) = \frac{\vec{V}_n}{1 + |\vec{V}_n| \eta (t - t_n)}$. We described the model using a four dimensional and non linear map $T(\theta_n, \alpha_n, |\vec{V}_n|, t_n) = (\theta_{n+1}, \alpha_{n+1}, |\vec{V}_{n+1}|, t_{n+1})$ where the dynamical variables are, respectively, the angular position of the particle; the angle that the trajectory of the particle forms with the tangent line at the position of the collision; the absolute velocity of the particle; and the instant of the hit with the boundary. Figure 1 illustrates the geometry of five successive collisions of the particle with the time-dependent boundary. To obtain the map, we start with an initial condition $(\theta_n, \alpha_n, |\vec{V}_n|, t_n)$. The Cartesian components of the boundary at the angular position (θ_n, t_n) are

$$X(\theta_n, t_n) = [A_0 + C \sin(t_n)] \cos(\theta_n), \quad (1)$$

$$Y(\theta_n, t_n) = [B_0 + C \sin(t_n)] \sin(\theta_n), \quad (2)$$

where A_0 and B_0 are constants, thus, at any time t_n we have elliptical shape. The control parameter $0 < C < \min(A_0, B_0)$ controls the amplitude of oscillation and $\theta \in [0, 2\pi)$ is a counterclockwise polar angle measured with respect to the positive horizontal axis. The angle between the tangent of the boundary at the position $(X(\theta_n), Y(\theta_n))$ measured with respect to the horizontal line is $\phi_n = \arctan \left[\frac{Y'(\theta_n, t_n)}{X'(\theta_n, t_n)} \right]$ where the expressions for both $X'(\theta_n, t_n) = dX(\theta_n, t_n)/d\theta_n$ and $Y'(\theta_n, t_n) = dY(\theta_n, t_n)/d\theta_n$. Since the expressions for ϕ_n and α_n are known, the angle of the trajectory of the particle measured with respect to the positive X-axis is $(\phi_n + \alpha_n)$. Such information allows us to write the particle's velocity vector as $\vec{V}_n = |\vec{V}_p(t)| [\cos(\phi_n + \alpha_n) \hat{i} + \sin(\phi_n + \alpha_n) \hat{j}]$. Where \hat{i} and \hat{j} denote the unity vectors with respect to the X and Y axis, respectively. The particle travels on a straight line until it hits the time dependent boundary. The position of the particle, as a function of time, for $t \geq t_n$, is $X_p(t) = X(\theta_n, t_n) + r(t) \cos(\phi_n + \alpha_n)$, $Y_p(t) =$

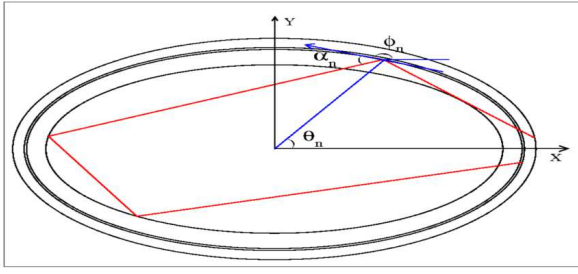


FIG. 1: Illustration of five collision with the time dependent boundary. The corresponding angles that describe the dynamics are also illustrated.

$Y(\theta_n, t_n) + r(t) \sin(\phi_n + \alpha_n)$. Where the sub-index p denotes that such coordinates correspond to the particle and $r(t) = \eta^{-1} \ln[1 + V_n \eta(t - t_n)]$, which is the displacement of the particle obtained from direct integration of $dr(t)/dt = \vec{V}_p(t)$. The distance of the particle measured with respect to the origin of the coordinate system is given by $R_p(t) = \sqrt{X_p^2(t) + Y_p^2(t)}$ and θ_p at $X_p(t), Y_p(t)$ is $\theta_p = \arctan[Y_p(t)/X_p(t)]$. Therefore, the angular position at $(n + 1)^{th}$ collision of the particle with the boundary, i.e. θ_{n+1} , is numerically obtained by solving the following equation $R_p(t) = \sqrt{X^2(\theta_p, t) + Y^2(\theta_p, t)}$. The time at $(n + 1)^{th}$ collision is obtained evaluating $t_{n+1} = t = t_n + t_c$, where t_c is the time during the flight. To obtain the new velocity we should note that the referential frame of the boundary is moving. Therefore, at the instant of collision, the following conditions must be obeyed

$$\vec{V}_{n+1} \cdot \vec{T}_{n+1} = \vec{V}_n \cdot \vec{T}_{n+1}, \quad (3)$$

$$\vec{V}_{n+1} \cdot \vec{N}_{n+1} = -\vec{V}_n \cdot \vec{N}_{n+1} + 2\vec{V}_b(t_{n+1}) \cdot \vec{N}_{n+1} \quad (4)$$

where the \vec{T} and \vec{N} are the unitary tangent and normal vectors, respectively, and the velocity of the boundary $\vec{V}_b(t_{n+1}) = C \cos(t_{n+1})[\cos(\theta_{n+1})\hat{i} + \sin(\theta_{n+1})\hat{j}]$. Then we have

$$|\vec{V}_{n+1}| = \sqrt{(\vec{V}_{n+1} \cdot \vec{T}_{n+1})^2 + (\vec{V}_{n+1} \cdot \vec{N}_{n+1})^2}. \quad (5)$$

Finally, the angle α_{n+1} is written as

$$\alpha_{n+1} = \arctan \left[\frac{\vec{V}_{n+1} \cdot \vec{N}_{n+1}}{\vec{V}_{n+1} \cdot \vec{T}_{n+1}} \right]. \quad (6)$$

With this four dimensional mapping, we can explore the dynamics of the model. However, before considering the time-dependent model let us illustrate the behaviour of the phase space for the static boundary. Indeed, it is well known that the ellipse is an integrable billiard system, the product of the two angular momenta with respect to the foci being the integral of motion [25, 26]. Figure 2, shows the phase space for $A_0 = 2$ and $B_0 = 1$. We can see a large double island limited by a separatrix and a set of invariant spanning curves. We can observe

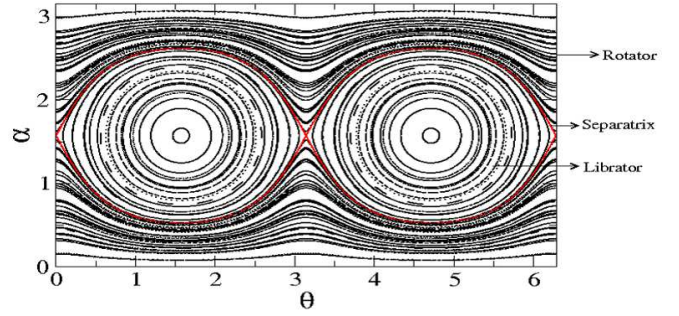


FIG. 2: Phase space for the static elliptical billiard. The control parameters: $A_0 = 2$ and $B_0 = 1$.

two different kinds of behaviour separated by a separatrix (red curve), namely, rotators and librators. Librators consist of trajectories that are confined between the two foci and in the phase space are confined by the separatrix curve. On the other hand, rotators are trajectories near to the boundary exploring all the values of θ . In the phase space they are outside of the separatrix curve.

As a part of our numerical results we shall discuss mainly the behaviour of the average velocity of the particle. Two different procedures were applied in order to obtain the average velocity. Firstly, we evaluate the average velocity over the orbit for a single initial condition and then over an ensemble of initial conditions. Hence, the average velocity is written as

$$\vec{V} = \frac{1}{M} \sum_{i=1}^M \frac{1}{n+1} \sum_{j=0}^n V_{i,j}, \quad (7)$$

where the index i corresponds to a sample of an ensemble of initial conditions, M denotes the number of different initial conditions. We have considered $M = 200$ in our simulations. It was shown by Lenz et al. [22, 23] that when a driving perturbation is introduced into the system, opposite to the expectations, it presents a phenomenon known as Fermi acceleration or unlimited energy gain. Such a behaviour happens because when the driving amplitude $C \neq 0$ the separatrix is replaced by a chaotic layer. A particle which starts its dynamics in a rotator orbit can change its dynamics to a liblator and vice versa. The chaotic diffusion within the chaotic layer leads to unlimited energy growth. Figure 3 shows the behavior of the average velocity as a function of the number of collisions. We have considered the conservative case where the drag coefficient is $\eta = 0$. For such a case the particle's velocity is $\vec{V}_p(t) = \vec{V}_n$ and $r(t) = |\vec{V}_n|(t - t_n)$. As one can see, all curves of the \vec{V} behave quite similarly in the sense that: (a) for short n , the average velocity remains constant for a while, but eventually, (b) after a crossover, all the curves start growing with the same exponent. This is at variance with the result obtained by Lenz et al [22], perhaps because they were not considering the average velocity for large enough values of n .

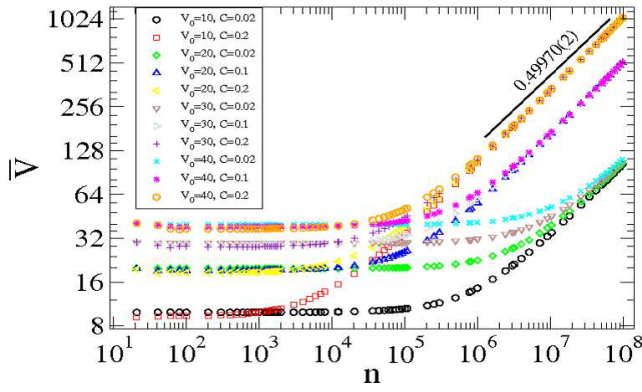


FIG. 3: Behaviour of \bar{V} vs. n for different initial velocities. The control parameters used were $A_0 = 2$, $B_0 = 1$. We have considered the coefficient of the drag force as $\eta = 0$.

We discuss now the effect of dissipation introduced via frictional force. To obtain the average velocity, we randomly choose $t \in [0, 2\pi]$, $\theta \in [0, 2\pi]$ and $\alpha \in [0, \pi]$. We also fix the value of $\eta = 10^{-3}$. Additionally, in order to avoid the initial plateau we also have fixed initial velocity as $V_0 = 10^{-5}$. The model of collisional dissipation by Leonel and Bunimovich [29] is different from our model of in-flight dissipation due to the drag force in detail, but should behave similarly in the statistical sense (on the average), especially in the chaotic regime, because then we have $\langle V_{n+1} \rangle = \langle V_n \rangle e^{-\eta r}$, thus the effective damping coefficient $\delta = e^{-\eta \langle r \rangle}$, where $\langle r \rangle$ is the mean free path of the particle.

In Fig. 4 (a) we show the behaviour of the average velocity as a function of the number of collisions for different values of C . Note that for different values of C and for short n , the average velocity starts to grow and then it bends towards a regime of saturation for long enough values of n . It must be emphasized that different values of the parameter C generate different behaviors for short n . However, applying the transformation $n \rightarrow nC^2$ coalesces all the curves at short n , as shown in Fig. 4(b). For such a behaviour, we can also propose the following scaling hypotheses: (i) When $n \ll n_x$ the average velocity is

$$\bar{V}(nC^2, C) \propto (nC^2)^\beta. \quad (8)$$

where the exponent β is called the acceleration exponent. (ii) When $n \gg n_x$, the average velocity is described as

$$\bar{V}_{sat} \propto C^\gamma. \quad (9)$$

where γ is the saturation exponent. (iii) The crossover from growth to the saturation is written as

$$n_x \propto C^z. \quad (10)$$

where z is called crossover exponent.

These scaling hypotheses allow us to describe the average velocity in terms of a scaling function of the type

$$\bar{V}[nC^2, C] = \lambda \bar{V}[\lambda^p nC^2, \lambda^q C], \quad (11)$$

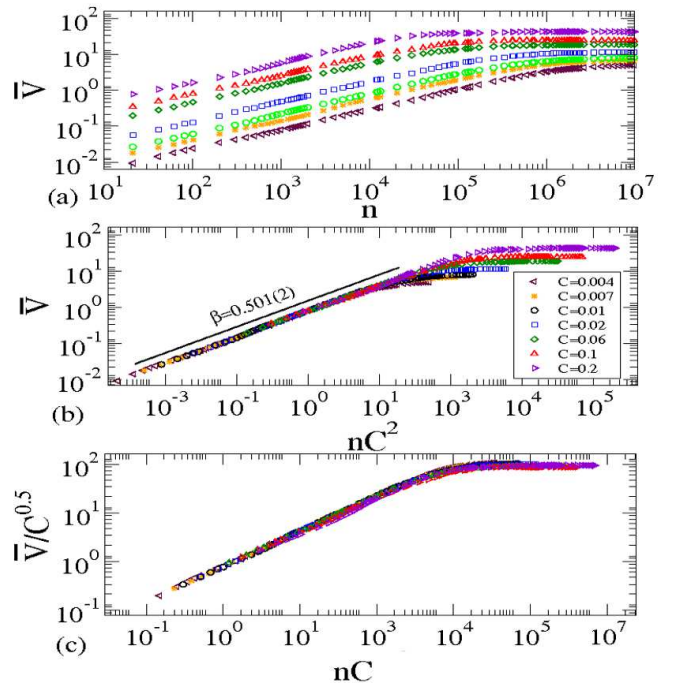


FIG. 4: (a) Behaviour of the average velocity as function of n for different values of the control parameter C . (b) Their initial collapse after the transformation nC^2 . (c) Their collapse onto a single universal plot.

where p and q are scaling exponents and λ is a scaling factor. Moreover, p and q must be related to β , γ and z . Because λ is a scaling factor, we can specify that $\lambda^p nC^2 = 1$, yielding

$$\bar{V}[nC^2, C] = (nC^2)^{-1/p} \bar{V}_1[n^{-q/p} C], \quad (12)$$

where $\bar{V}_1[(nC^2)^{-q/p} C] = \bar{V}[1, (nC^2)^{-q/p} C]$ is assumed to be constant for $n \ll n_x$. Comparing Eqs. (8) and (12), we obtain $\beta = -1/p$. Choosing now $\lambda^q C = 1$, we find that $\lambda = C^{-1/q}$ and Eq. (11) is given by

$$\bar{V}[nC^2, C] = C^{-1/q} \bar{V}_2[C^{-p/q} nC^2], \quad (13)$$

where $\bar{V}_2[C^{-p/q} nC^2] = \bar{V}[C^{-p/q} nC^2, 1]$ is assumed to be constant for $n \gg n_x$. Comparing Eqs. (9) and (13), we obtain $\gamma = -1/q$ [see Fig. 5 (a)]. A power law fitting in Fig. 5 gives us that $\beta = 0.501(2)$. Such value was obtained from the range of $C \in [10^{-3}, 2 \times 10^{-1}]$. Given the two values of the scaling factor λ , one can easily conclude that $z = \frac{\gamma}{\beta} - 2 = -0.97(1)$, which is in excellent agreement with the value obtained numerically, as shown in Fig. 5 (b). A confirmation of the initial hypotheses is made by a collapse of all the curves of \bar{V} vs. n onto a single and universal plot, as shown in Fig. 4 (c), showing that the system is scaling invariant under specific transformation. With this good collapse of all the curves of the average velocity and considering that the critical exponents are $\beta \cong 0.5$, $\gamma \cong 0.5$ and $z \cong -1$, we can conclude that the time dependent driven elliptical billiard belongs to the same class of universality of the one

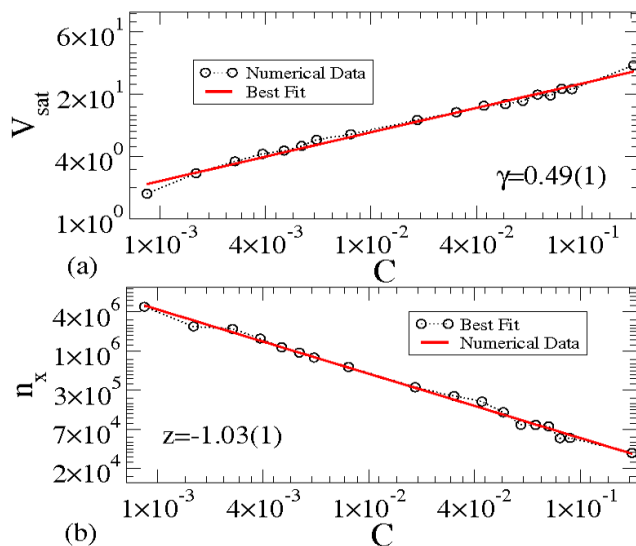


FIG. 5: (a) Plot of \bar{V}_{sat} as function of the control parameter C . (b) Behaviour of the crossover number n_x against C .

dimensional Fermi-Ulam model [27] and the periodically corrugated waveguide [28]. The scaling can also be described in terms of the coefficient of the drag force η . In such a case $V_{sat} \propto \eta^{-0.521(3)}$ and $n_x \propto \eta^{-1.070(6)}$. We have fixed $C = 0.1$ and $V_0 = 10^{-5}$. Therefore, $\eta \rightarrow 0$ implies that V_{sat} and n_x both diverge, thus recovering the

results for the conservative case, i.e., exhibiting Fermi acceleration. Additionally, our results reinforce that in-flight dissipation is a sufficient condition to suppress the phenomenon of Fermi acceleration like in the case of collisional dissipation [29].

As the concluding remark, we have studied some dynamical properties of a time dependent driven elliptical billiard. In the static case the phase space is integrable where two kinds of trajectories are observed: rotator and librator. We have introduced time dependent perturbations and in-flight dissipation. We have observed that average velocity grows for small number of collision and then, after a crossover, it reaches a regime of saturation for large n . Thus we do not observe the unlimited energy growth (Fermi acceleration). We have also studied the behaviour of the average velocity using scaling arguments. We have shown that there is a relation between the critical exponents γ , β and z . Our scaling hypotheses are confirmed by a perfect collapse of all the curves onto a single universal plot. Additionally, we confirm that the two dimensional elliptical model belongs to the same class of universality of the Fermi-Ulam model (1-D) and the corrugated wave guide (1-D), for the range of control parameters studied.

D.F.M.O gratefully acknowledges Ad futura Foundation - Slovenia for financial support. M. R. acknowledges the financial support of The Slovenian Research Agency.

-
- [1] G. Katz, M. A. Ratner, R. Kosloff, Phys. Rev. Lett. 98, 203006 (2007).
- [2] S. E. Sklarz, D. J. Tannor, N. Khaneja, Phys. Rev. A 69, 053408 (2004)
- [3] V. L'vov, A. Pomyalov, I. Procaccia, V. Tiberkevich, Phys. Rev. Lett. 92, 244503 (2004).
- [4] P. Parmananda, M. Hildebrand, M. Eiswirth, Phys. Rev. E 56, 239 (1997).
- [5] J. K. Bhattacharjee, D. Thirumalai, Phys. Rev. Lett. 67, 196 (1991).
- [6] M. N. Shneider, P. F. Barker, Phys. Rev. A 71, 053403(1-9) (2005).
- [7] R. Gommers, S. Bergamini, F. Renzoni, Phys. Rev. Lett. 95, 073003 (2005).
- [8] M. Steiner, M. Freitag, V. Perebeinos, J. C. Tsang, J. P. Small, M. Kinoshita, D. Yuan, J. Liu, P. Avouris, Nature Nanotechnology 4, 320 (2009)
- [9] Y. Zhao, C. Ma, G. Chen, Q. Jiang, Phys. Rev. Lett. 91, 175504 (2003).
- [10] W. V. Liu, W. C. Schieve, Phys. Rev. Lett. 78, 3278 (1997).
- [11] K. Tsumura, T. Kunihiro, Phys. Lett. B 668, 425 (2008).
- [12] H.-J. Stöckmann, *Quantum Chaos: An Introduction* (Cambridge University, Cambridge, England, 1999)
- [13] C. Dembowski, H. D. Graf, A. Heine, T. Hesse, H. Rehfeld, A. Richter, Phys. Rev. Lett. 86, 3284 (2001).
- [14] F. Libisch, S. Rotter, J. Güttinger, C. Stampfer, J. Burgdörfer, Phys. Rev. B 79, 115423 (2009).
- [15] M. F. Andersen, A. Kaplan, T. Grünzweig, N. Davidson, Phys. Rev. Lett. 97, 104102 (2006).
- [16] E. Fermi, Phys. Rev. 75, 1169 (1949).
- [17] A. Loskutov, A.R. Ryabov, L.G. Akinshin, J. Phys. A 33, 7973 (2000)
- [18] E. D. Leonel, D. F. M. Oliveira, A. Loskutov, Chaos, 19, 033142 (2009).
- [19] E. D. Leonel, L. Bunimovich, Phys. Rev. E, 82, 016202 (2010).
- [20] A. B. Ryabov, A. Loskutov, J. Phys. A, 43, 125104 (2010).
- [21] D. F. M. Oliveira, J. Vollmer, E. D. Leonel, accepted for publication in Physica D.
- [22] F. Lenz, F. K. Diakonov, and P. Schmelcher, Phys. Rev. Lett. 100, 014103 (2008).
- [23] F. Lenz, F. K. Diakonov, and P. Schmelcher, Phys. Rev. E 76, 066213 (2007).
- [24] J. Koiller, R. Markarian, S. M. O. Kamphorst, S. P. de Carvalho, J. Stat. Phys., 83, 127 (1996).
- [25] M. V. Berry, Eur.J.Phys. 2, 91 (1981).
- [26] Y. G. Sinai *Introduction to Ergodic Theory* (Princeton University Press, Princeton, New Jersey, 1976)
- [27] E. D. Leonel, P. V. E. McClintock, J. k. L. Silva, Phys. Rev. Lett. 93, 14101 (2004).
- [28] E. D. Leonel, Phys. Rev. Lett. 98, 114102 (2007).
- [29] E. D. Leonel, L. A. Bunimovich, Phys. Rev. Lett. 104, 224101 (2010).